Using the LU Recombination Method to Extend the Application of Circuit-Oriented Finite Element Methods to Arbitrarily Low Frequencies

Haixin Ke, *Member, IEEE*, Todd H. Hubing, *Fellow, IEEE*, and Francescaromana Maradei, *Senior Member, IEEE*

***Abstract*—The circuit-oriented finite-element method (FEM) is a method that combines a finite-element field solver with a circuit analyzer and is suitable for analyzing electromagnetic field/circuit coupled problems. This paper describes a significant improvement to existing circuit-oriented FEMs that reduces the number of circuit elements and eliminates low-frequency stability problems. A modified LU recombination method is used to reformulate the original field-solver matrix equations. Circuits based on the reformulated equations are relatively insensitive to numerical errors and do not contain the small-value series resistors that circuit solvers are normally forced to add in order to guarantee a stable solution. Using this approach, the circuit-oriented FEM is capable of time- and/or frequency-domain simulations of problems containing linear or nonlinear lumped elements over a wide bandwidth. Examples are provided that demonstrate the ability of the new technique to model geometries from dc to several gigahertz in a single simulation.**

***Index Terms*—Finite-element method (FEM), low frequency, LU recombination, SPICE.**

I. Introduction

FULL-WAVE 3-D electromagnetic (EM) simulation techniques such as the finite-element method (FEM), the finite-difference time-domain (FDTD) method, and the method of moments (MoM) are widely used to analyze microwave components and circuits. Field solvers based on full-wave modeling techniques generally have difficulty modeling certain lumped circuit elements, especially nonlinear components. Pure circuit simulators, although very powerful and efficient in many circumstances, cannot model full-wave EM interactions very well. Combining full-wave EM and circuit simulation in a single analysis technique offers many advantages, and several numerical tools for analyzing field-circuit coupled problems have been developed [1]–[6]. The circuit-oriented FEM technique [3]–[6] combines the flexible mesh generation and analysis capabilities of the FEM with the fast solution capabilities of circuit solvers such as SPICE. This approach is well suited for analyzing problems that involve complex distributed EM geometries, as well as lumped circuit elements. However, because it is derived from a full-wave FEM formulation, the circuit-oriented FEM is hampered by low-frequency instability problems and cannot be used to analyze low-frequency problems or geometries driven by a source signal that has a dc component.

Full-wave EM simulation algorithms suffer from low-frequency instability due to the decoupling of the electric and magnetic fields at low frequencies. The problem related to the FEM and MoM was analyzed in [7] and [8]. The physical meaning of the low-frequency instability is different in the FEM and MoM. However, these instabilities can be explained mathematically in the same manner in terms of their matrix formulations. The matrix formulations can be viewed as a sum of two parts. The first part scales linearly with frequency, and therefore, is very small at low frequencies. The second part dominates at low frequencies and is singular. The overall matrix is poorly conditioned at low frequencies and the information of the first part can be obscured by numerical error in the second part when the two parts are summed. The LU recombination method proposed in [7] and [8] enforces the singularity property of the second part in a manner that ensures that the information contained in the first part will not be neglected when the two parts are added. The method works very well for both FEM and MoM modeling techniques.

In the circuit-oriented FEM, referred to as FEM-SPICE in this paper, the singular part of the FEM matrix is represented by inductors and the nonsingular part is represented by resistors and capacitors. Small numerical errors in the singular part create undesired inductive connections in the circuit model. These "error" connections appear as combinations of inductors rather than single elements so it is difficult to identify them in the circuit. The equivalent inductances are large enough that they do not affect the high frequency behavior of the circuit, but they affect the circuit simulation at low frequencies, causing inaccurate and unstable results. In addition, circuit simulators such as SPICE add small resistors to avoid closed inductor loops in the circuit. These resistors are usually added in series with the inductors. These artificial resistors exacerbate the effect of the numerical errors and create undesired resistive connections that are mixed with the error inductive connections. The LU recombination method described in [7] can be used to adjust the FEM matrix formulation to remove the effect of

Manuscript received August 03, 2009; revised August 29, 2009. First published April 19, 2010; current version published May 12, 2010.

H. Ke was with the Department of Electrical and Computer Engineering, Clemson University, Clemson, SC 29634 USA. He is now with the Department of Biomedical Engineering, Washington University, St. Louis, MO 63130 USA (e-mail: keh@seas.wustl.edu).

T. H. Hubing is with the Department of Electrical and Computer Engineering, Clemson University, Clemson, SC 29634 USA (e-mail: hubing@clemson.edu).

F. Maradei is with the Department of Electrical Engineering, University of Rome "La Sapienza," 00184 Rome, Italy (e-mail: francesca.maradei@uniroma1.it).

Color versions of one or more of the figures in this paper are available online at http://ieeexplore.ieee.org.

Digital Object Identifier 10.1109/TMTT.2010.2045533

numerical error on the inductor values, but it cannot account for the artificial resistors in the circuit implementation. Thus, a new strategy is required to make the method applicable to the FEM-SPICE model.

In this paper, the low-frequency limitations of the FEM-SPICE method are explored. The LU recombination method is reformulated to modify the FEM matrix in a way that not only removes the numerical errors in the inductances, but also eliminates the artificial resistors. This significantly reduces the number of components in the SPICE simulations and produces circuits that accurately model full-wave problem geometries from dc to the highest valid frequencies of the original FEM formulation.

Section II briefly describes the FEM-SPICE model. The low-frequency problem with the model is explained and a new implementation of the LU recombination method in FEM-SPICE is described. Numerical results are then presented to validate the method.

II. FEM-SPICE Modeling

The FEM [9] is well suited for solving problems involving inhomogeneous arbitrarily shaped objects. It is usually used to solve the vector Helmholtz equation in terms of the electric field

$$\nabla \times \left(\frac{\nabla \times \mathbf{E}(\boldsymbol{r})}{j\omega\mu_0\mu_r} \right) + j\omega\varepsilon_0\varepsilon_r \mathbf{E}(\boldsymbol{r}) = -\mathbf{J}^{\text{int}}(\boldsymbol{r}) - \frac{1}{j\omega\mu_0\mu_r} \nabla \times \mathbf{M}^{\text{int}}(\boldsymbol{r}) \quad (1)$$

where $\mathbf{J}^{\text{int}}$ and $\mathbf{M}^{\text{int}}$ are impressed electric and magnetic sources. ω is the angular frequency. μ_0 and ε_0 are the free-space permeability and permittivity, and μ_r and ε_r are the relative permeability and permittivity.

The unknown $\mathbf{E}$ field is expanded using basis functions $\boldsymbol{w}_n(\boldsymbol{r})$ as

$$\mathbf{E}(\boldsymbol{r}) = \sum_n E_n \boldsymbol{w}_n(\boldsymbol{r}) \quad (2)$$

where E_n are unknown coefficients representing the field strengths along the edges of the finite elements. A similar set of functions is applied as weighting functions to (1), and the equation is discretized into a matrix form

$$\mathbf{A}\,\mathbf{E} = \mathbf{B}\,\mathbf{J} + \mathbf{S} \quad (3)$$

where $\mathbf{E}$ is a vector containing the unknown coefficients in (2). The right-hand side of (3) represents the boundary conditions and the source terms. A detailed description of $\mathbf{B}$, $\mathbf{J}$, and $\mathbf{S}$ is provided in [10]. For simplicity, the contribution of the boundary integral will be neglected in this paper. The elements of $\mathbf{A}$ are then

$$[\mathbf{A}]_{mn} = \int_V \left[\frac{(\nabla \times \boldsymbol{w}_{\boldsymbol{n}}(\boldsymbol{r})) \cdot (\nabla \times \boldsymbol{w}_{\boldsymbol{m}}(\boldsymbol{r}))}{j\omega\mu_0\mu_r} + j\omega\varepsilon_0\varepsilon_r \boldsymbol{w}_{\boldsymbol{n}}(\boldsymbol{r}) \cdot \boldsymbol{w}_{\boldsymbol{m}}(\boldsymbol{r}) \right] dV. \quad (4)$$

The system of (3) is similar in structure to multiport network equations based on admittance matrix representations. Each edge of an FEM tetrahedral element corresponds to a port in the circuit network; and each row in $\mathbf{A}$ represents the admittance of the circuit components connected to that port. The admittance is composed of two parts ($\mathbf{A}_1$ and $\mathbf{A}_2$) where

$$[\mathbf{A}_1]_{mn} = \int_V j\omega\varepsilon_0\varepsilon_r \boldsymbol{w}_{\boldsymbol{n}}(\boldsymbol{r}) \cdot \boldsymbol{w}_{\boldsymbol{m}}(\boldsymbol{r})\, dV \quad (5a)$$

and

$$[\mathbf{A}_2]_{mn} = \int_V \frac{(\nabla \times \boldsymbol{w}_{\boldsymbol{n}}(\boldsymbol{r})) \cdot (\nabla \times \boldsymbol{w}_{\boldsymbol{m}}(\boldsymbol{r}))}{j\omega\mu_0\mu_r} dV. \quad (5b)$$

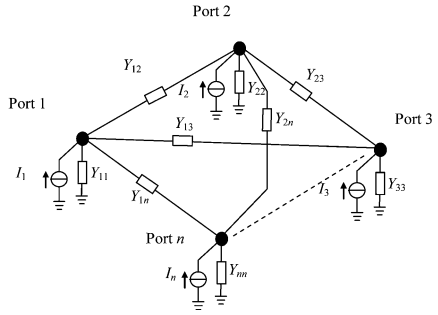

Fig. 1. Circuit representation of FEM matrix equation.

The elements of $\mathbf{A}_1$ behave like capacitors and the elements of $\mathbf{A}_2$ behave like inductors. This suggests that the $\mathbf{A}$ matrix can be represented by a circuit composed of parallel LC branches. The $\mathbf{E}$ vector in (3) represents the unknown port voltages to be solved. The $\mathbf{S}$ vector represents the current sources at the ports. Therefore, the FEM matrix (3) can be translated into an equivalent-circuit model, as shown in Fig. 1. This equivalent-circuit model has been described in [5] and [6]. In [6], the $\mathbf{A}$ matrix was translated into an admittance matrix directly. In [5], the $\mathbf{A}$ matrix was normalized by the lengths of the edges of the tetrahedral finite elements. In both cases, voltages obtained from the solution of the circuit model correspond to the electric field along a corresponding finite-element edge.

The LC parallel branches do not model any loss. Dielectric loss can be included in (4) by adding a frequency-independent term. This term can be modeled in the circuit by adding resistors in parallel with the inductors and capacitors.

III. Low-Frequency Instability in FEM-SPICE Modeling

The low-frequency problem inherent in full-wave FEMs has been addressed in [7]. On one hand, the elements in matrix $\mathbf{A}_1$ approach zero at arbitrarily low frequencies, as seen from (5a), and their contribution tends to be lost in numerical error during the summation of $\mathbf{A}_1$ and $\mathbf{A}_2$. On the other hand, the matrix $\mathbf{A}_2$ in (5b) was shown to be singular when using the popular lowest order curl-conforming basis functions. It has N_l sets of linearly dependent rows, where N_l is equal to the total number of internal nodes in the finite-element mesh [11]. The condition number of $\mathbf{A}$ gets large at low frequencies where $\mathbf{A}_2$ dominates. Therefore, the loss of information in $\mathbf{A}_1$, although very small, leads to large errors in the solution at low frequencies.

The FEM-SPICE model has a similar low-frequency problem because the circuit model is directly derived from the FEM matrix formulation. In the FEM-SPICE model, the contributions from the $\mathbf{A}_1$ and $\mathbf{A}_2$ matrices are represented by capacitors

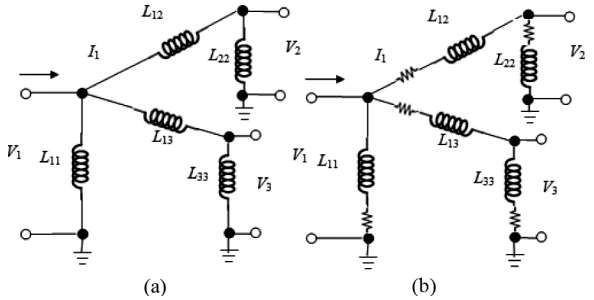

Fig. 2. Simple circuit model. (a) Mathematical representation. (b) Circuit implementation in SPICE.

and inductors, respectively. The capacitors derived from the $\mathbf{A}_1$ matrix have stable values that are independent of frequency. Low-frequency instability problems in the SPICE model are the result of the inductors derived from the $\mathbf{A}_2$ matrix.

This can be explained using the simple three-port network shown in Fig. 2(a), where only inductors are considered for simplicity. The voltage–current relation at Port 1 can be written as

$$\frac{1}{j\omega}\left(\frac{1}{L_{11}}+\frac{1}{L_{12}}+\frac{1}{L_{13}}\right)\cdot V_1-\frac{1}{j\omega L_{12}}V_2-\frac{1}{j\omega L_{13}}V_3=I_1. \tag{6}$$

If the inductors connected to Port 1 are related by

$$\frac{1}{L_{11}}=-\frac{1}{L_{12}}-\frac{1}{L_{13}} \tag{7}$$

then the current I_1 flowing into Port 1 is independent of the port voltage V_1. In this case, the port voltage could be any value no matter what the port current is. However, small numerical errors in the values of the inductors would mean that (7) is not strictly enforced. This would cause the admittance term associated with the port voltage V_1, i.e., $1/j\omega$ times the term in the brackets in (6), to have a finite value instead of zero. This undesired admittance is the result of the errors in the values of the three inductors. It is not explicitly represented by a circuit element in the model, but it effectively behaves like an inductor connecting Port 1 to ground. For small numerical errors, the value of the equivalent inductor is so large that it does not affect the high-frequency behavior of the circuit. However, at arbitrarily low frequencies, the equivalent inductance shorts Port 1 and forces the solution for the port voltage V_1 to be zero.

It has been shown in [7] that if there is an inner node in the finite-element mesh, the rows in the matrix $\mathbf{A}_2$ are not linearly independent. When the rows are translated into inductors, the inductors have a relationship similar to (7). Therefore, the FEM-SPICE model derived from a finite-element formulation with inner nodes will have subcircuits similar to that shown in Fig. 2(a). The numerical errors will create "error" inductances that cause sets of inductors that are supposed to represent open circuits to have the impedance of a short circuit resulting in unrealistic solutions.

Another problem with the solution of circuits like the one in Fig. 2(a) is that SPICE circuit solvers do not allow closed loops consisting entirely of inductors. A resistor must be added in the loop to ensure the stability of the solution. Generally a small fixed-value resistor is added in series with each inductor, as shown in Fig. 2(b). These artificial resistors add numerical errors that are insignificant as long as the resistance is smaller than the impedance of the inductor. Accounting for the effect of these resistors, (6) would be rewritten as

$$\left(\frac{1}{R_a+j\omega L_{11}}+\frac{1}{R_a+j\omega L_{12}}+\frac{1}{R_a+j\omega L_{13}}\right)\cdot V_1-\frac{1}{R_a+j\omega L_{12}}V_2-\frac{1}{R_a+j\omega L_{13}}V_3=I_1 \tag{8}$$

where R_a is a small resistance. The resistors in series with L_{11}, L_{12}, and L_{13} become problematic even if the resistance is smaller than the impedance of the three inductors because, with these resistors present, it is not possible to make the admittance associated with the port voltage V_1 in (8) zero, even when the errors associated with the inductors are removed.

IV. LU Recombination Method in FEM-SPICE Model

A new approach based on the LU recombination method is proposed to generate an FEM-SPICE model that works at both high and low frequencies. The approach uses the LU recombination method to determine which rows in the matrix $\mathbf{A}_2$ are linearly dependent. For each group of dependent rows, the approach then creates a new row that removes the numerical errors. Since the new row is a linear combination of the dependent rows, it can replace any row within the group. The proposed approach also generates a combination matrix that records all the dependent rows and how they are linearly related. This matrix is used to incorporate lumped elements and obtain the final solution.

The detailed process is described using the following example. Let $\boldsymbol{a}_{1i}$ and $\boldsymbol{a}_{2i}$, $(i=1,2,\ldots,N)$ denote the rows of the $\mathbf{A}_1$ and $\mathbf{A}_2$ matrices, respectively (e.g., $\boldsymbol{a}_{13}$ is a vector representing the third row of the matrix $\mathbf{A}_1$). Here, N is the total number of edges. Assume rows 1–3 are linearly dependent such that

$$\boldsymbol{a}_{21}+\boldsymbol{a}_{22}+\boldsymbol{a}_{23}=\mathbf{0}. \tag{9}$$

where $\mathbf{0}$ is an $N\times 1$ zero vector. The LU recombination method described in [7] is used to locate these groups of dependent rows. At the same time, it generates an $N\times 1$ combination vector $\boldsymbol{c}=\{1,1,1,0,\ldots,0\}^T$, where the superscript T denotes the transpose, which indicates that the summation of the first three rows in $\mathbf{A}_2$ creates a zero vector. Combining these three rows generates a new row vector

$$\begin{aligned}\boldsymbol{a}_0&=\boldsymbol{a}_{10}+\boldsymbol{a}_{20}\\&=(\boldsymbol{a}_{11}+\boldsymbol{a}_{12}+\boldsymbol{a}_{13})+(\boldsymbol{a}_{21}+\boldsymbol{a}_{22}\boldsymbol{a}_{23})\cdot\\&=c^T\,(\mathbf{A}_1+\mathbf{A}_2).\end{aligned} \tag{10}$$

This new row is called a zero-edge row because ideally $\boldsymbol{a}_{20}$ is zero. It is used to replace any of the first three rows; in this case, say, the first row. The column vector is also replaced to maintain the symmetry. This is done by the following matrix multiplication:

$$\mathbf{A}^{\text{new}}=\begin{bmatrix}c^T\\ \mathbf{0}\quad\mathbf{I}\end{bmatrix}[\mathbf{A}_1+\mathbf{A}_2]\begin{bmatrix}c\quad\mathbf{0}^T\\ \mathbf{I}\end{bmatrix} \tag{11}$$

where $\mathbf{I}$ denotes an $(N-1)\times(N-1)$ identity matrix and $\mathbf{0}$ is an $(N-1)\times 1$ zero vector. In practice, the matrix multiplication is performed only on the matrix $\mathbf{A}_1$; the first row and column of

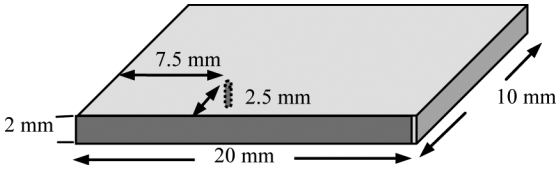

Fig. 3. Geometry of a power bus structure.

the matrix $\mathbf{A}_2$ are set to zero directly. The zero-edge elements have no inductive admittance, and therefore, circuit models created from the modified admittance matrix $\mathbf{A}^{\text{new}}$ do not have inductors that correspond to these elements or their associated artificial resistors. This effectively removes both the "error" inductances and resistances that will affect the low-frequency solution. For each group of dependent rows in $\mathbf{A}_2$, one row in $\mathbf{A}$ is replaced by the zero edge, and all necessary replacements are performed using the matrix multiplication shown in (11). Unlike the original LU recombination method, this new approach does not recover the original finite-element matrix, but instead creates a new one.

The new FEM formulation can be expressed in terms of the original formulation as

$$\mathbf{A}^{\text{new}}\,\mathbf{E}^{\text{new}} = \mathbf{S}^{\text{new}} \tag{12a}$$

or

$$\begin{bmatrix} c^T \\ \mathbf{0} \quad \mathbf{I} \end{bmatrix} [\mathbf{A}_1 + \mathbf{A}_2] \begin{bmatrix} c & \mathbf{0}^T \\ & \mathbf{I} \end{bmatrix} \mathbf{E}^{\text{new}} = \begin{bmatrix} c^T \\ \mathbf{0} \quad \mathbf{I} \end{bmatrix} \mathbf{S}. \tag{12b}$$

The new FEM formulation can be translated into a circuit for SPICE simulation using traditional FEM-SPICE techniques. Circuits created from the new formulation will not suffer from low-frequency instability. Note that the linear combination is also applied to the source vector so extra source elements may be added to the new circuit model. Since the FEM matrix $\mathbf{A}$ is changed, the solution is also changed. The combination matrix $\begin{bmatrix} c & \mathbf{0}^T \\ & \mathbf{I} \end{bmatrix}$ can be used to recover the intended solution as

$$\mathbf{E} = \begin{bmatrix} c^T \\ \mathbf{0} \quad \mathbf{I} \end{bmatrix} \mathbf{E}^{\text{new}}. \tag{13}$$

V. Numerical Results

To utilize the LU recombination method, the FEM matrix elements have to be normalized by the length of the edges, as done in [5]. Thus, a formulation similar to [5] is used in this paper.

The first example used to validate the approach described in the previous sections is the circuit board power bus model shown in Fig. 3. The structure is composed of two metal planes and a dielectric substrate. The size of the planes is 20 mm × 10 mm, and they are modeled as perfect electric conductors. The dielectric substrate between the two planes has a thickness of 2 mm and a relative permittivity of 4.4. The board is excited by an ideal current source located 2.5 and 7.5 mm from the edges at one corner. There is a 50-Ω source resistor in parallel with the source. The fringing field was neglected and the four sidewalls of the board were modeled as perfect magnetic conductors.

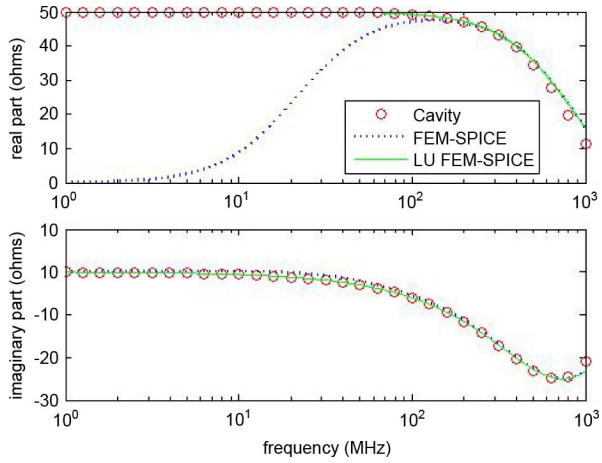

Fig. 4. Input impedance of the power bus structure.

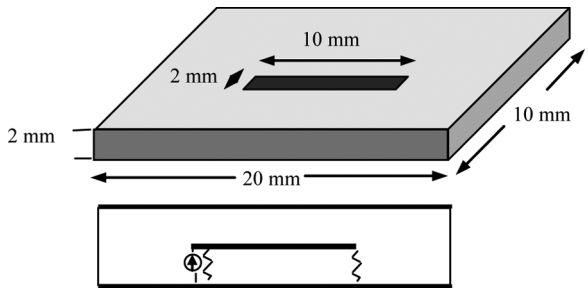

Fig. 5. Geometry of the trace between two metal planes.

The input impedance was calculated using different methods and the results are shown in Fig. 4. The results obtained using a cavity model [12] are used as a reference since the cavity model yields accurate results for this type of structure over the entire frequency range evaluated. The dotted line is the result obtained using a normal FEM-SPICE model. The solid line is the result obtained using FEM-SPICE with the LU recombination corrections described in Section IV. The normal FEM-SPICE results behave as if the planes were shorted at low frequencies. After LU recombination, the calculated input impedance matches the cavity model result very well.

A second example, shown in Fig. 5, is a trace between two planes in a circuit board. The board is the same as the one in the first example. A 10 × 1 mm trace is located in the middle of the board, 1 mm from both metal planes. The trace is driven by a 50-Ω source between one end of the trace and the lower plane. It is terminated by a 50-Ω resistor at the opposite end.

The complex input impedance of the trace was calculated by three methods: FEM, FEM-SPICE, and FEM-SPICE with LU recombination. The large dots in Fig. 6 show the result of the FEM simulation. The results begin to be unstable below 20 MHz. The error becomes large below 1 MHz. The dotted line shows the results obtained using the normal FEM-SPICE model. In the model, SPICE places 10-$\mu\Omega$ resistors in series with the inductors. The results start to degrade at several hundred megahertz and the trace is shorted by the error inductors at

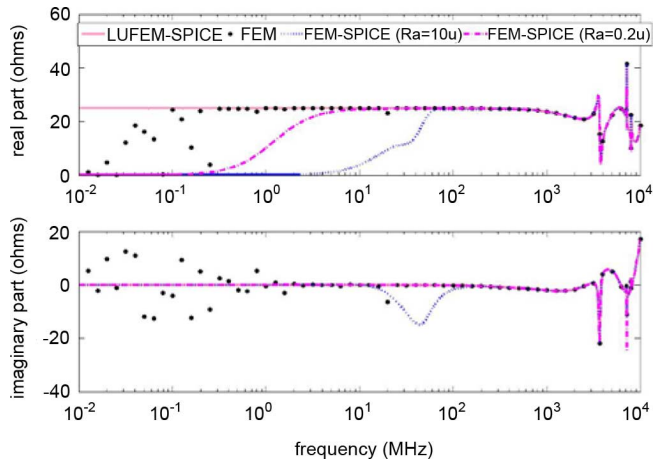

Fig. 6. Input impedance of a trace between two planes.

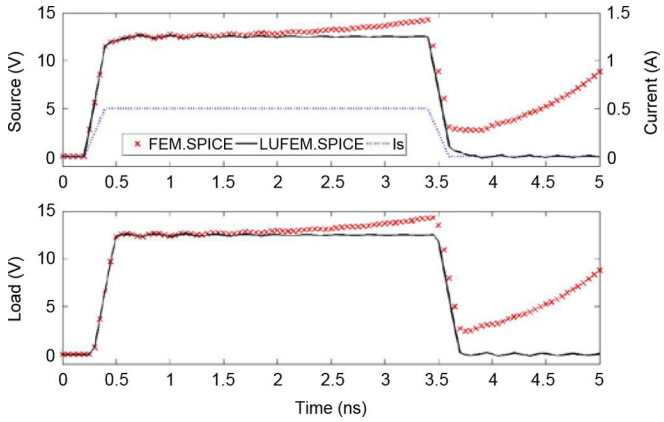

Fig. 7. Time-domain response of the trace between two planes.

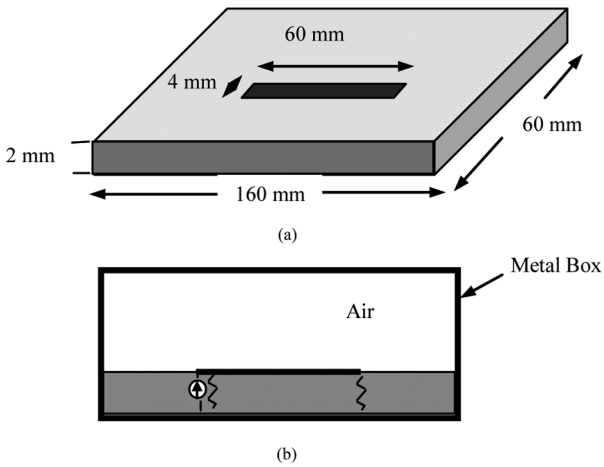

Fig. 8. Metal box example. (a) Substrate with trace. (b) Enclosed by metal box.

frequencies below 3 MHz. The dashed line shows another result obtained using the normal FEM-SPICE model with smaller (0.2-$\mu\Omega$) resistors. The improvement in the second SPICE model indicates that using a smaller resistor yields a better result, but does not solve the problem. The results obtained using FEM-SPICE with LU recombination, indicated by the solid line, are correct over the entire frequency range.

Circuits created by FEM-SPICE models usually have components with negative values. These circuits can be unstable when performing a transient (i.e., time domain) analysis. Dependent sources were introduced in the models above to replace the negative components, as described in [5]. The idea is to determine the currents through the negative components using controlled sources and the absolute value of the components in a separate circuit, and then reverse the direction of the currents in the main circuit. This replacement does not affect the LU recombination method. The LU recombination method is applied to the model before introducing these dependent sources.

Fig. 7 shows the voltages across the source and load resistors in the previous example in response to a trapezoidal input. The input waveform has a period of 5 ns with a delay of 0.2 ns. The rise and fall times are 0.2 ns and the duration is 3 ns. The input current waveform is shown in Fig. 7 via the dotted line. The voltages at the source and load end of the trace are plotted separately. The results of the FEM-SPICE model with LU recombination show the correct steady-state voltages and a delay of about 70 ps between the source and load signals, corresponding to the length of the trace. Without the LU recombination correction, the FEM-SPICE results are initially accurate, but do not exhibit a stable steady-state solution.

The third example is a dielectric substrate with a metal trace on it that is enclosed in a metal box, as shown in Fig. 8. The substrate has dimensions of $160 \times 60 \times 2$ mm and a dielectric constant of 4.4. The trace is 60-mm long and 4-mm wide. The height of the metal box is 8 mm. A 50-Ω source is placed at one end of the trace. A 50-Ω resistor is placed at the other end.

In this configuration, there are two materials in the computational domain, i.e., the dielectric substrate and the air above it. The trace input impedance calculated by FEM-SPICE with and without LU recombination are compared in Fig. 9. Fig. 10 shows the time-domain voltage responses at the source and load ends, when the source signal is a trapezoidal wave with a risetime of 50 ps and a period of 5 ns. The result with LU recombination is stable, while the result without LU recombination becomes unstable after a couple of cycles. This example demonstrates that material properties affect the value of the FEM matrix elements, but they do not change the linear relationships between the rows of the matrix. The LU recombination method is applicable to configurations containing different materials without additional modification.

VI. Discussion

The FEM-SPICE technique described in this paper does not exhibit a one-to-one correspondence between FEM edge elements and SPICE circuit nodes because the FEM admittance matrix is rearranged before it is converted to a circuit. The solution for the original ports can be obtained by multiplying the combination matrix in (11) by the solution obtained with the new model. However, it is important to note that the voltages corresponding to the zero edges are not changed by the multiplication of the combination matrix. When analyzing multiport systems, it is possible to preserve the edge-to-node correlations of particular ports by ensuring that the rows corresponding to

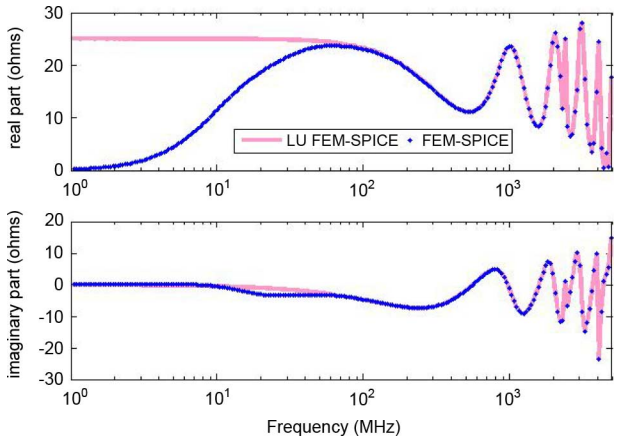

Fig. 9. Input impedance of the trace in a metal box.

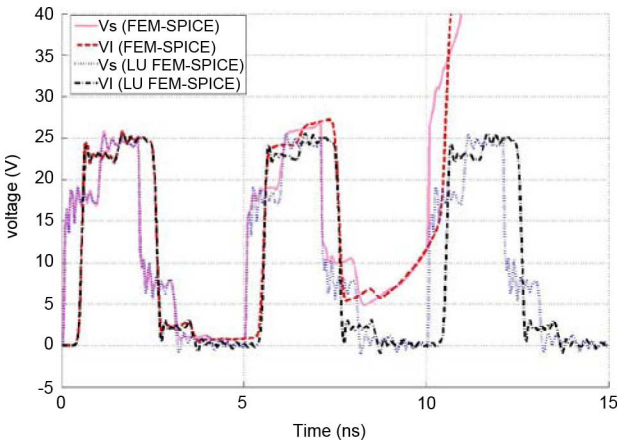

Fig. 10. Time-domain response of the trace in a metal box.

these ports are replaced by the zero edges during the LU recombination process. The voltages calculated by the circuit model at these ports do not need extra processing.

The FEM-SPICE model is suitable for analyzing field/circuit coupled problems. It is straightforward to add linear or nonlinear circuit elements to the circuit model after it is generated. However, the linear combination of (11) changes the original FEM matrix, and therefore, redefines the ports of the circuit. If the lumped element is a linear component such as a resistor or capacitor, it can be added to the FEM matrix before the LU recombination. If the lumped element is nonlinear or described by behavior models, a zero-edge port should be defined at the lumped-element location to ensure that the identity of this port is not redefined by the LU recombination process.

VII. Conclusions

FEM-SPICE is a mixed EM field and circuit analysis technique that combines the advantages of the FEM and circuit solvers and is well suited for analyzing field-circuit coupled problems. Traditional FEM-SPICE techniques do not work at low frequencies due to numerical instabilities in the FEM formulation and small value resistors that are inserted by SPICE simulators. In this paper, the LU recombination method is applied to FEM-SPICE models in a manner that eliminates the effect of small numerical errors and prevents the unintended insertion of undesired resistors. The new FEM-SPICE formulation works well in frequency-domain simulations at arbitrarily low frequencies and can also be used for both dc and transient analyses.

The results presented here were obtained from a full-wave FEM formulation that solves for the electric field. At low frequencies, where the electric and magnetic fields become more decoupled, the solution approaches its electrostatic value. For problems where low-frequency magnetic field interactions are critical, it would be more appropriate to start with a full-wave FEM formulation that solves for the magnetic field strength.

References

[1] M. Feliziani and F. Maradei, "Modeling of electromagnetic fields and electrical circuits with lumped and distributed elements by the WETD method," *IEEE Trans. Magn.*, vol. 35, no. 3, pp. 1666–1669, May 1999.

[2] K. Guillord, M.-F. Wong, V. F. Hanna, and J. Citerne, "A new global time-domain electromagnetic simulator of microwave circuits including lumped elements based on finite-element method," *IEEE Trans Microw. Theory Tech.*, vol. 47, no. 10, pp. 2045–2048, Oct. 1999.

[3] M. Feliziani and F. Maradei, "FEM solution of time-harmonic electromagnetic fields by an equivalent electrical network," *IEEE Trans. Magn.*, vol. 34, no. 3, pp. 1666–1669, Jul. 2000.

[4] M. Feliziani and F. Maradei, "Circuit-oriented FEM: Solution of circuit-field coupled problems by circuit equations," *IEEE Trans. Magn.*, vol. 38, no. 2, pp. 965–968, Mar. 2002.

[5] C. Guo and T. Hubing, "Circuit models for power bus structures on printed circuit boards using a hybrid FEM-SPICE method," *IEEE Trans. Adv. Packag.*, vol. 29, no. 3, pp. 441–447, Aug. 2006.

[6] F. Maradei, H. Ke, and T. Hubing, "Full-wave model of frequency dispersive media by circuit-oriented FEM," *IEEE Trans. Electromagn. Compat.*, vol. 51, no. 2, pp. 312–319, May 2009.

[7] H. Ke and T. Hubing, "Low-frequency full-wave finite element modeling using the LU recombination method," *Appl. Comput. Electromagn. Soc. J.*, vol. 23, no. 4, pp. 303–308, Dec. 2008.

[8] H. Ke and T. Hubing, "A modified LU recombination technique for improving the performance of boundary element methods at low frequencies," *Appl. Comput. Electromagn. Soc. J.*, vol. 20, no. 3, pp. 178–185, Nov. 2005.

[9] J. Jin, *The Finite Element Method in Electromagnetics*. New York: Wiley, 1993.

[10] Y. Ji and T. Hubing, "EMAP5: A 3D hybrid FEM/MOM code," *Appl. Comput. Electromagn. Soc. J.*, vol. 15, no. 1, pp. 1–12, Mar. 2000.

[11] N. Venkatarayalu, M. Vouvakis, Y. Gan, and J. Lee, "Suppressing linear time growth in edge element based finite element time domain solution using divergence free constraint equation," in *Proc. IEEE AP-S Int. Symp.*, Jul. 2005, vol. 4b, pp. 193–196.

[12] G. T. Lei, R. W. Techentin, and B. K. Gilbert, "High-frequency characterization of power/ground-plane structures," *IEEE Trans. Microw. Theory Tech.*, vol. 47, no. 5, pp. 562–569, May 1999.

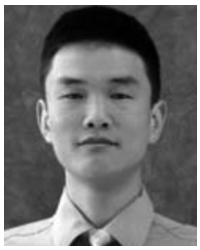

Haixin Ke (M'06) received the B.S. and M.S. degrees from Tsinghua University, Beijing, China, in 1998 and 2001, respectively, and the Ph.D. degree from the University of Missouri–Rolla, in 2006, all in electrical engineering.

From 2006 to 2009, he was a Postdoctoral Researcher with Clemson University, Clemson, SC. He is currently a Postdoctoral Research Associate with the Department of Biomedical Engineering Washington University, St. Louis, MO. His research interests include computational electromagnetics, EM compatibility, and microwave/optical imaging.

Todd H. Hubing (S'82–M'82–SM'93–F'96) received the BSEE degree from the Massachusetts Institute of Technology (MIT), Cambridge, the M.S.E.E. degree from Purdue University, West Lafayette, IN, and the Ph.D. degree from North Carolina State, Raleigh.

Following seven years with IBM and 17 years with the University of Missouri–Rolla, he joined Clemson University in 2006 as the Michelin Professor for Vehicular Electronics.

Prof. Hubing is a Fellow of the Applied Computational Electromagnetics Society. He was the 2002–2003 President of the IEEE Electromagnetic Compatibility (EMC) Society and continues to serve on the Board of Directors as vice president for communication services.

Francescaromana Maradei (M'96–SM'06) received the Laurea degree in electrical engineering (*cum laude*) fromthe University of Rome "La Sapienza," Rome, Italy, the Diplome d'Etudes Approfondies in electrical engineering from the Institut National Polytecnique de Grenoble, Grenoble, France, and the Ph.D. degree in electrical engineering from the University of Rome "La Sapienza."

In 1996, she joined the Department of Electrical Engineering, University of Rome "La Sapienza," where she is currently an Associate Professor.

Prof. Maradei has been a member of the Editorial Board of the IEEE Conference on Electromagnetic Field Computation (CEFC) and the IEEE COMPUMAG Conference since 1998. She is currently the President of the IEEE Electromagnetic Compatibility Society.